

Projectile-charge-state dependence of target L -shell ionization by 1.86-MeV/amu fluorine and silicon ions and 1.8-MeV/amu chlorine ions

F. D. McDaniel, A. Toten, R. S. Peterson, J. L. Duggan, S. R. Wilson, and J. D. Gressett
Department of Physics, North Texas State University, Denton, Texas 76203

P. D. Miller
Oak Ridge National Laboratory, Oak Ridge, Tennessee 37830

Grzegorz Lapicki
Department of Physics, New York University, New York, New York 10003
 (Received 31 July 1978)

$L\alpha$ x-ray-production cross sections have been measured for solid targets of ${}_{60}\text{Nd}$, ${}_{67}\text{Ho}$, and ${}_{79}\text{Au}$ for 1.86-MeV/amu ${}_{9}\text{F}$ and ${}_{14}\text{Si}$, and 1.8-MeV/amu ${}_{17}\text{Cl}$ ions as a function of the incident charge state. From the projectile-charge-state dependence of the cross sections, both direct-ionization and electron-capture contributions were extracted for a comparison to Coulomb ionization theories. The data provide supporting evidence for the theory of electron capture with a reduced binding effect. With standard fluorescence and Coster-Kronig yields uncorrected for multiple-ionization effects, the direct ionization theories did not simultaneously reproduce the projectile- Z_1 and target- Z_2 dependences of the data.

I. INTRODUCTION

X-ray-production data^{1,2} for both the K and L shells have been shown to be in good agreement with the direct-ionization (DI) theory³⁻⁶ when the ratio of projectile atomic number (Z_1) to target atomic number (Z_2) is small, i.e., $Z_1/Z_2 \ll 1$. This theory accounted for the Coulomb deflection and, in the perturbed-stationary state (PSS) theory, for the increased binding and polarization effects. The Coulomb perturbed stationary state (CPSS) approach considers direct ionization to the continuum and is independent of projectile charge state.

In addition to DI, for $Z_1/Z_2 \lesssim 1$, electron capture (EC) to bound states of the projectile must also be considered.^{7,8} Calculations of target inner-shell ionization through EC by heavy incident ions have recently been reported.⁹ The calculations employ the analytical expressions of Nikolaev,¹⁰ which are derived with observed binding energies and screened hydrogenic wave functions in the Oppenheimer¹¹-Brinkman-Kramers¹² (OBK) approximation and in the low-velocity regime include modifications for increased target electron binding energy and Coulomb deflection effects analogous to those employed for DI.³⁻⁶ In this theory, the increase in the binding energy due to the presence of the projectile was obtained by an integration over all impact parameters. We have shown for the K shell that as the ratio of projectile velocity (v_1) to target-electron orbital velocity (v_{2K}) approaches one, this procedure overesti-

mates the binding effect.¹³ The increased binding to the target should be of importance only when the projectile is within the electronic shell of interest. Therefore, as has been assumed in the CPSS theory, for direct ionization^{4,6} we assume there is no increase in binding for projectiles at impact parameters larger than a predetermined cutoff radius. This cutoff radius is chosen to be given by the expectation value of the radial distance in the L shell, which is equal to $\frac{3}{2}$ and $\frac{5}{4}$ of the hydrogenic L -shell radius in the $2s$ and $2p$ and states, respectively.

We reported measurements of the projectile charge-state dependence of K -shell ionization by silicon ions.¹³ Very good agreement was found between the observed projectile charge-state dependence of the x-ray production cross sections and the CPSS theory for direct ionization⁴ and the EC theory⁹ with the reduced binding effect.¹³ We extend these measurements to the L shell. We have determined the $L\alpha$ x-ray production cross sections for thin solid targets of ${}_{60}\text{Nd}$, ${}_{67}\text{Ho}$, and ${}_{79}\text{Au}$ by ions (with incident charge states q) of ${}_{9}\text{F}$ ($q=5-9$), ${}_{14}\text{Si}$ ($q=7-14$), and ${}_{17}\text{Cl}$ ($q=9-16$). The energy per unit mass was 1.86 MeV/amu for ${}_{9}\text{F}$ and ${}_{14}\text{Si}$ and 1.8 MeV/amu for ${}_{17}\text{Cl}$. A large increase in the target cross sections was observed for projectiles with K -shell vacancies, which is attributable to electron capture from the L shell of the target to the K shell of the projectile. These measurements are compared to the direct ionization theories^{6,14} and the electron-capture theory⁹ with the reduced-binding effect.¹³

II. EXPERIMENTAL PROCEDURES AND DATA ANALYSIS

Fluorine, silicon, and chlorine ions in different incident charge states were obtained from the EN Tandem Van de Graaff accelerator at ORNL. The high incident charge states were produced with N_2 gas or carbon foil strippers placed in the beam line and selected by magnetic analysis. Target L -shell x-ray emission was detected in a Si(Li) spectrometer having a resolution of ~ 180 eV at 5.94 keV.

Since the primary emphasis of the experiments was the projectile charge-state dependence of the L -shell ionization, good statistics were obtained only for the $L\alpha_1$ and $L\alpha_2$ x rays. The $L\alpha = L\alpha_1 + L\alpha_2$ x-ray yields were systematically extracted using the peak fitting routine SAMPO.¹⁵ Absolute $L\alpha$ x-ray production cross sections were determined by normalizing the x-ray yields to the Rutherford-scattered ion yield. Details of the experimental procedures and data analysis are discussed elsewhere.¹⁶

III. RESULTS AND DISCUSSION

X-ray production cross sections were determined for solid targets that were thin enough that the target-thickness dependence of the x-ray yields was minimized. To ensure that the cross sections were indeed independent of target thickness, measurements were made for solid targets of different thicknesses with incident-ion charge states of $q = 5$ for $^{19}\text{F}^{+q}$ and $q = 7$ for $^{28}\text{Si}^{+q}$. These measurements showed that the target thickness dependence¹⁷ of the apparent $\sigma_{L\alpha}$ cross section began to appear for

thicknesses greater than $\sim 50 \mu\text{g}/\text{cm}^2$. To minimize this effect, only target thicknesses less than $12 \mu\text{g}/\text{cm}^2$ were used in the cross-section measurements.

The measured $L\alpha$ x-ray production cross sections are given in Table I with the target thicknesses and the incident ion charge states. The absolute uncertainties associated with the x-ray production cross sections have been discussed earlier.¹⁸ For the present data these uncertainties are given in Table I and are generally less than 9% for the ^{19}F and ^{28}Si data and less than 13% for the ^{35}Cl data. Because the ^{35}Cl ($q = 16$) ion beam current was small, the uncertainty in the x-ray intensity was $\sim 25\%$. Also given in Table I are the Z_1/Z_2 ratios and the ratio of the projectile velocity (v_1) to the average L -shell electron orbital velocity (v_{2L}) for these data.

Figure 1 shows the projectile charge state dependence of the ^{60}Nd $L\alpha$ x-ray production cross section for $^{28}\text{Si}^{+q}$ ions. The $\sigma_{L\alpha}$ is essentially independent of projectile charge state for ^{28}Si ions (fully filled circles) without K -shell vacancies ($q = 8-11$). This independence of projectile charge state is just what one would expect from the direct ionization theories such as the CPSS theory.³⁻⁶ For ^{28}Si ions with K -shell vacancies ($q = 13, 14$), one observes an enhancement of the $\sigma_{L\alpha}$ for ^{60}Nd due to additional L -shell vacancies in neodymium which is believed to be produced by EC from the L shell of the target atom to the K shell of the ^{28}Si ion. The enhancements for the hydrogenlike ^{28}Si ions (half-filled circle) and fully stripped ^{28}Si ions (open circle) are factors of ~ 3.5 and ~ 7.1 , respec-

TABLE I. Target $L\alpha$ x-ray production cross sections in barns, Z_1/Z_2 ratios, and v_1/v_{2L} ratios for $^{19}\text{F}^{+q}$, $^{28}\text{Si}^{+q}$, and $^{35}\text{Cl}^{+q}$ ions of different incident charge state q on thin solid targets of ^{60}Nd , ^{67}Ho , and ^{79}Au of thickness ρt . Numbers in parenthesis denote powers of 10, e.g., $6.8 \pm 0.5(3) = (6.8 \pm 0.5) \times 10^3$.

	1.86 MeV/amu $^{19}\text{F}^{+q}$		
	^{60}Nd	^{67}Ho	^{79}Au
Z_1/Z_2	0.150	0.134	0.114
v_1/v_{2L}^a	0.31	0.27	0.23
ρt^b	2.6	1.7	1.8
q	$\sigma_{L\alpha}$ (Nd)	$\sigma_{L\alpha}$ (Ho)	$\sigma_{L\alpha}$ (Au)
5	$6.8 \pm 0.5(3)$	$2.3 \pm 0.2(3)$	$5.3 \pm 0.4(2)$
6	$6.6 \pm 0.5(3)$	$2.6 \pm 0.2(3)$	$5.6 \pm 0.4(2)$
7	$6.7 \pm 0.5(3)$	$2.5 \pm 0.2(3)$	$5.8 \pm 0.4(2)$
8	$8.1 \pm 0.7(3)$	$2.8 \pm 0.2(3)$	$6.6 \pm 0.6(2)$
9	$9.5 \pm 0.8(3)$	$3.0 \pm 0.2(3)$	$7.4 \pm 0.7(2)$
$\bar{\sigma}_{L\alpha}^c$	$6.7 \pm 0.5(3)$	$2.5 \pm 0.2(3)$	$5.5 \pm 0.4(2)$
$\sigma_{L\alpha}(8) - \bar{\sigma}_{L\alpha}^d$	$1.4 \pm 0.7(3)$	$0.4 \pm 0.3(3)$	$1.1 \pm 0.7(2)$
$\sigma_{L\alpha}(9) - \bar{\sigma}_{L\alpha}^e$	$2.8 \pm 0.9(3)$	$0.6 \pm 0.3(3)$	$2.0 \pm 0.8(2)$

TABLE I. (Continued)

1.86 MeV/amu $^{28}_{14}\text{Si}^{+q}$			
	^{60}Nd	^{67}Ho	^{79}Au
Z_1/Z_2	0.233	0.209	0.177
v_1/v_{2L}^a	0.31	0.27	0.23
ρt^b	2.6 ^f	1.7 ^g	11.8
q	$\sigma_{L\alpha}$ (Nd)	$\sigma_{L\alpha}$ (Ho)	$\sigma_{L\alpha}$ (Au)
7	1.6 ± 0.1(4)	8.0 ± 0.6(3)	1.3 ± 0.1(3)
8	1.5 ± 0.1(4)	9.4 ± 0.7(3)	1.2 ± 0.1(3)
9	1.5 ± 0.1(4)	7.9 ± 0.6(3)	1.2 ± 0.1(3)
10	1.5 ± 0.1(4)	6.5 ± 0.5(3)	1.2 ± 0.1(3)
11	1.6 ± 0.1(4)	6.0 ± 0.5(3)	1.2 ± 0.1(3)
12	2.6 ± 0.2(4)	8.5 ± 0.7(3)	1.7 ± 0.1(3)
13	5.4 ± 0.5(4)	2.1 ± 0.2(4)	2.8 ± 0.2(3)
14	1.1 ± 0.1(5)	2.9 ± 0.3(4)	4.3 ± 0.4(3)
$\bar{\sigma}_{L\alpha}^c$	1.6 ± 0.1(4)	7.6 ± 0.6(3)	1.2 ± 0.1(3)
$\sigma_{L\alpha}(13) - \bar{\sigma}_{L\alpha}^d$	3.8 ± 0.5(4)	1.3 ± 0.2(4)	1.6 ± 0.3(3)
$\sigma_{L\alpha}(14) - \bar{\sigma}_{L\alpha}^e$	9.6 ± 1.4(4)	2.1 ± 0.3(4)	3.1 ± 0.4(3)
1.8 MeV/amu $^{35}_{17}\text{Cl}^{+q}$			
	^{60}Nd		
Z_1/Z_2	0.283		
v_1/v_{2L}^a	0.38		
ρt^b	4.6		
q	$\sigma_{L\alpha}$ (Nd)		
9	2.2 ± 0.2(4)		
10	2.9 ± 0.4(4)		
11	2.3 ± 0.4(4)		
12	2.4 ± 0.3(4)		
13	2.4 ± 0.3(4)		
14	2.3 ± 0.3(4)		
15	3.1 ± 0.4(4)		
16	9.5 ± 2.3(4)		
$\bar{\sigma}_{L\alpha}^c$	2.4 ± 0.3(4)		
$\sigma_{L\alpha}(16) - \bar{\sigma}_{L\alpha}^d$	7.1 ± 2.3(4)		

^aThe ratio of projectile velocity (v_1) to L -shell electron orbital velocity (v_{2L}) is given by $v_1/v_{2L} = (E_1 n^2 / \lambda Z_{2L}^2 R)^{1/2}$, where E_1 is the projectile laboratory energy, λ is the ratio of projectile mass to the electron mass, n is the principal quantum number ($n=2$ for the L shell), $R=13.6$ eV is the Rydberg, and $Z_{2L} = Z_2 - 4.15$ is the screened target nuclear charge.

^b ρt is the target thickness in $\mu\text{g}/\text{cm}^2$ with the target mounted at 45° to the incident beam direction.

^cArithmetic averages of the cross sections ($\bar{\sigma}_{L\alpha}$) are given for the x-ray-production data obtained for all projectile charge states $q \leq Z_1 - 3$. The averages were determined for the ions (charge states): $^{19}\text{F}^{+q}$ ($q=5,6$), $^{28}\text{Si}^{+q}$ ($q=7-11$), $^{35}\text{Cl}^{+q}$ ($q=9-14$). Since for these data the projectiles possessed no K -shell vacancies, and since L -shell to L -shell electron capture is negligible, these averages represent DI cross sections.

^dThe contributions to the target x-ray-production cross sections due to electron capture by a projectile with one K -shell vacancy are determined as $\sigma_{L\alpha}(q=Z_1-1) - \bar{\sigma}_{L\alpha}(q \leq Z_1-3)$.

^eThe contributions to the target x-ray-production cross sections due to electron capture for a projectile with two K -shell vacancies are determined as $\sigma_{L\alpha}(q=Z_1) - \bar{\sigma}_{L\alpha}(q \leq Z_1-3)$.

^fFor the data taken with a $^{28}\text{Si}^{+q}$ ion beam, the ^{60}Nd target thickness was $2.6 \mu\text{g}/\text{cm}^2$ for the $q=7-13$ charge states and $4.6 \mu\text{g}/\text{cm}^2$ for the $q=14$ charge state.

^gFor the data taken with a $^{28}\text{Si}^{+q}$ ion beam, the ^{67}Ho target thickness was $1.7 \mu\text{g}/\text{cm}^2$ for the $q=7-13$ charge states and $9.3 \mu\text{g}/\text{cm}^2$ for the $q=14$ charge state.

tively. The small enhancement in the cross section of 1.7, for the $q=12$ state, might be due to the production of metastable states (e.g., $1s2s\ ^3\text{S}_1$)

in the heliumlike $^{28}_{14}\text{Si}$ ions as they pass through the carbon stripper foil prior to magnetic analysis.¹⁹ The projectile charge-state dependences observed

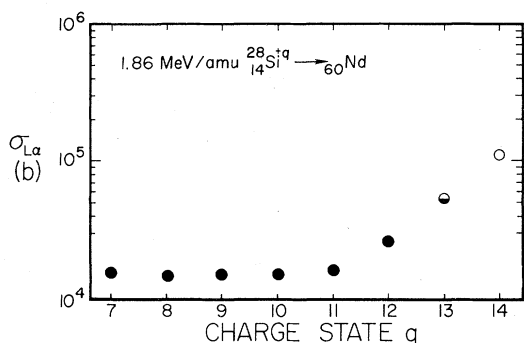


FIG. 1. Projectile-charge-state dependence of ${}_{60}\text{Nd}$ $L\alpha$ x-ray-production cross sections for 1.86 MeV/amu ${}_{14}^{28}\text{Si}^{+q}$ ions. The cross sections were measured for targets thin enough to exhibit no apparent thickness dependence. The meaning of the symbols is discussed in the text and their size corresponds to experimental uncertainties.

for the other projectile target combinations are essentially the same as that observed for ${}_{14}^{28}\text{Si}^{+q}$ ions on ${}_{60}\text{Nd}$. The enhancements in the $L\alpha$ cross sections were found to be larger for increasing

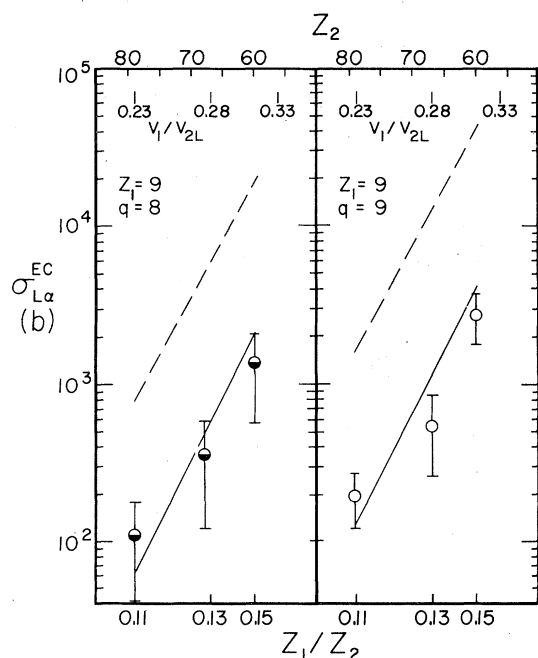


FIG. 2. Inferred $L\alpha$ x-ray-production cross sections for ${}_{60}\text{Nd}$, ${}_{67}\text{Ho}$, and ${}_{79}\text{Au}$ due to EC for incident hydrogenlike ($q=8$) and fully stripped ($q=9$) ${}_{9}^{19}\text{F}^{+q}$ ions at 1.86 MeV/amu. The Nikolaev OBK calculations (Ref. 10) are represented by the dashed line. The solid line represents the EC calculations of Lapicki and Losnky (Ref. 9) with modification for Coulomb deflection and reduced binding effect as described in Ref. 13.

Z_1/Z_2 ratios which is expected since the K -shell binding energy of the projectile becomes more nearly matched to the L -shell binding energy of the target atom.

The inferred EC contributions to target L -shell vacancy production and therefore to target $L\alpha$ x-ray production are determined by subtracting the average direct ionization data ($q \leq Z_1 - 3$) from the data obtained for hydrogenlike ($q = Z_1 - 1$) or fully stripped ($q = Z_1$) incident ions. The averages of the data obtained for projectiles with no K -shell vacancies were determined for the ions (charge states) as follows: ${}_{9}^{19}\text{F}^{+q}$ ($q = 5, 6$), ${}_{14}^{28}\text{Si}^{+q}$ ($q = 7-11$), and ${}_{17}^{35}\text{Cl}^{+q}$ ($q = 9-14$). The averages of the $L\alpha$ x-ray production cross sections representing direct ionization and the $L\alpha$ x-ray cross sections due to EC are given in Table I.

The inferred $L\alpha$ x-ray production cross sections for ${}_{60}\text{Nd}$, ${}_{67}\text{Ho}$, and ${}_{79}\text{Au}$ due to EC for hydrogenlike ($q=8$) and fully stripped ($q=9$) ${}_{9}^{19}\text{F}^{+q}$ ions at 1.86 MeV/amu are shown in Fig. 2. The data are presented as a function of Z_2 , Z_1/Z_2 , and v_1/v_{2L} and demonstrate that the EC contributions for a particular ion species (Z_1) at a fixed velocity v_1 increase with increasing Z_1/Z_2 and v_1/v_{2L} or decreasing Z_2 . The dashed line in Fig. 2 shows the EC cross sections obtained from the expressions given by Nikolaev¹⁰ in the OBK approximation. The Nikolaev OBK calculations exceed the data by an order of magnitude. The solid line represents the low-velocity EC calculations of Lapicki and Losnky⁹ with the Coulomb deflection and, as suggested earlier for the K -shell,¹³ the reduced binding effect. The agreement with the measurements is considerably improved. The $L\alpha$ x-ray production cross sections were calculated from the ionization cross sections for the i th subshell of the L shell using values of the fluorescence yields (ω_i) and Coster-Kronig yields (f_{ij}) recommended by Krause²⁰ and the radiative widths (Γ) of Scofield.²¹ The $L\alpha$ x-ray production cross section ($\sigma_{L\alpha}$) is related to the subshell ionization cross section (σ_{L_i} , $i = 1, 2, 3$) by the expression

TABLE II. Fluorescence and Coster-Kronig yields^a and the ratios of radiative rates.^b

	${}_{60}\text{Nd}$	${}_{67}\text{Ho}$	${}_{79}\text{Au}$
ω_3	0.125	0.182	0.320
f_{12}	0.190	0.190	0.140
f_{13}	0.300	0.300	0.530
f_{23}	0.152	0.142	0.122
$\Gamma_\alpha/\Gamma_{L3}$	0.815	0.807	0.777

^a From Ref. 20.

^b From Ref. 21.

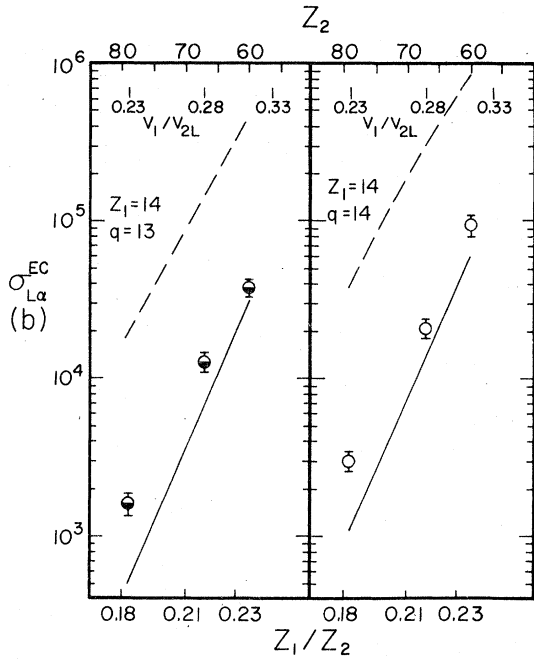


FIG. 3. Inferred $L\alpha$ x-ray-production cross sections for ${}_{60}\text{Nd}$, ${}_{67}\text{Ho}$, and ${}_{79}\text{Au}$ due to electron capture for incident hydrogenlike ($q=13$) and fully stripped ($q=14$) ${}_{14}^{28}\text{Si}^{+q}$ ions at 1.86 MeV/amu. The theoretical curves are described in Fig. 2 and in the text. Note that the error bars are larger in the previous figure because of the smaller difference in $\sigma_{L\alpha}$ ($q=Z_1, Z_1-1$) - $\bar{\sigma}_{L\alpha}$ for fluorine ions.

$$\sigma_{L\alpha} = \omega_3 [\sigma_{L_3} + f_{23}\sigma_{L_2} + (f_{13} + f_{12}f_{23})\sigma_{L_1}] \Gamma_\alpha / \Gamma_{L_3}. \quad (1)$$

The fluorescence yields, Coster-Kronig yields, and the ratios of radiative rates used to determine $\sigma_{L\alpha}$ are given in Table II. These yields are not corrected for multiple ionization effects.

Figure 3 shows the inferred $L\alpha$ x-ray-production cross sections for ${}_{60}\text{Nd}$, ${}_{67}\text{Ho}$, and ${}_{79}\text{Au}$ due to EC for hydrogenlike ($q=13$) and fully stripped ($q=14$) ${}_{14}^{28}\text{Si}^{+q}$ ions at 1.86 MeV/amu. The Nikolaev OBK calculations¹⁰ are given by the dashed line and exceed the data by an order of magnitude. The solid line represents the EC calculations of Lapicki and Losonsky⁹ as modified to include Coulomb deflection and partially increased binding-energy effects.¹³ The agreement between the data and the EC calculations that include the binding-energy and and Coulomb-deflection effects is much improved when compared with the predictions of Ref. 10, although the data are underestimated for smaller v_1/v_{2L} ratios.

Figure 4 shows the Z_1 dependence of the EC contribution to the $L\alpha$ x-ray-production cross sec-

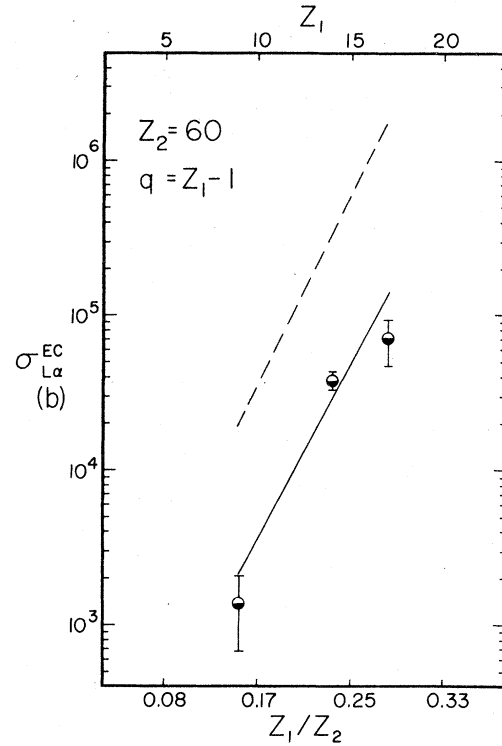


FIG. 4. Z_1 dependence of the electron capture contribution to the ${}_{60}\text{Nd}$ $L\alpha$ x-ray-production cross section for incident hydrogenlike ${}_{9}^{19}\text{F}$ and ${}_{14}^{28}\text{Si}$ ions at 1.86 MeV/amu and ${}_{17}^{35}\text{Cl}$ ions at 1.8 MeV/amu. The theoretical curves are described in Fig. 2 and in the text.

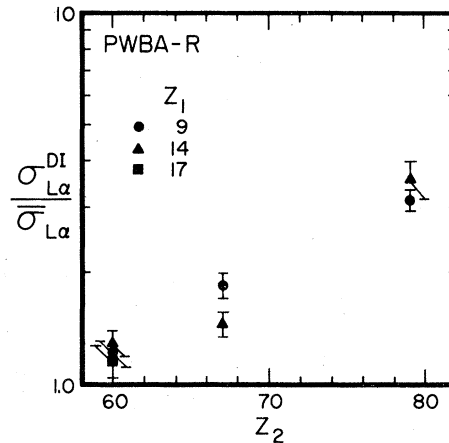


FIG. 5. Ratios of the PWBA-R theoretical direct-ionization x-ray cross sections ($\sigma_{L\alpha}^{\text{DI}}$) to the experimental $L\alpha$ x-ray cross sections as a function of target atomic number Z_2 . The experimental cross sections are given in Table I as arithmetic averages ($\bar{\sigma}_{L\alpha}$) of the data obtained for projectiles without K -shell vacancies, which were found to be independent of projectile charge state. The data are compared to the PWBA (Ref. 14) with an approximate correction for relativistic (R) target electron velocities (Ref. 22). The relationship between ionization and x-ray production cross sections is given by Eq. (1) using the parameters in Table II.

tions of ${}_{60}\text{Nd}$ for hydrogenlike ions of ${}^{19}\text{F}$ and ${}^{28}\text{Si}$ at 1.86 MeV/amu and ${}^{35}\text{Cl}$ at 1.8 MeV/amu. The EC data are seen to increase with increasing Z_1 for a particular target species. The dashed line represents the Nikolaev OBK calculations that overpredict the data by an order of magnitude. The solid line is based on the EC calculations of Lapicki and Losonsky⁹ that account for the Coulomb deflection and partial¹³ increased binding energy effects and are found to provide much better representations of the data.

While this theory is found to provide good estimates of the EC data for a range of Z_1 and Z_2 , the same cannot be said for the DI theories. As discussed earlier, the DI results are represented by the average of the target x-ray cross section data for projectiles *without* K -shell vacancies. Since L -shell to K -shell EC is not possible and L -shell to L -shell EC contributes at most 10% to ionization,⁹ these average data are assumed to represent the DI contribution to x-ray production by the target atom.

The average data that are independent of projectile charge state are compared to the plane-wave Born-approximation (PWBA)-R DI theory in Fig. 5 for all projectile-target combinations investigated. The ratio of the DI theory to experiment is presented as a function of Z_2 of the target atom.

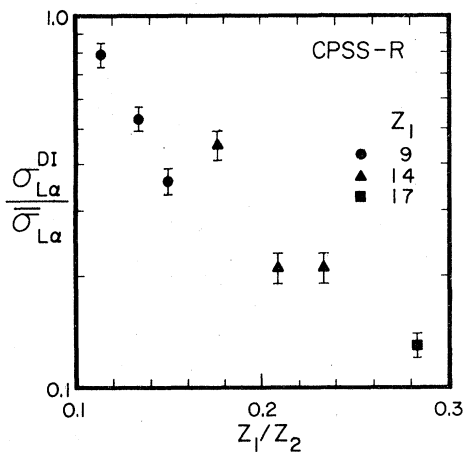


FIG. 6. Ratios of the CPSS-R theoretical direct-ionization x-ray cross sections ($\sigma_{L\alpha}^{DI}$) to the experimental $L\alpha$ x-ray cross section as a function of Z_1/Z_2 . The experimental cross sections are given in Table I as arithmetic averages ($\bar{\sigma}_{L\alpha}$) of the data obtained for projectiles without K -shell vacancies which were found to be independent of projectile charge state. The data are compared to the nonrelativistic PSS theory with Coulomb (C) deflection (Ref. 6) multiplied by the relativistic (R) correction factors (Ref. 22).

Ideally this ratio should be equal to the value of one. In Fig. 5 the data are compared to the PWBA results of Choi, Merzbacher, and Khandelwal¹⁴ with an approximate correction for relativistic target electron velocities as described by Hansen.²² The relativistic correction, which consists of a multiplicative factor to the cross sections determined in the binary encounter approximation,²² has been applied to the PWBA cross sections in the present work and labeled PWBA-R. This correction increased the theoretical cross sections by the following factors for a particular projectile (Z_1)-target (Z_2) combination (Z_1, Z_2): 1.04 (9, 60), 1.07 (9, 67), 1.15 (9, 79), 1.05 (14, 60), 1.09 (14, 67), 1.20 (14, 79), 1.07 (17, 60). The Z_1 dependence in the cross sections are essentially the same for the range of targets investigated. The PWBA-R provides better agreement with the data for the lower- Z_2 targets.

In Fig. 6, the average data that are independent of projectile charge state are compared to the CPSS theory of Brandt and Lapicki.^{5,6} The nonrelativistic results of this calculation have also been multiplied by the approximate relativistic correction factors given above and are labeled CPSS-R. In Fig. 6, the ratios of the DI theory to experiment is presented as a function of Z_1/Z_2 . The Z_1 dependence in the cross sections is no longer the same for the different target atoms studied. The CPSS-R theory underpredicts the data for all targets by increasing amounts with increasing Z_1/Z_2 . The CPSS-R theory provides better agreement for the higher- Z_2 targets in contrast to that observed with the PWBA-R theory. The comparison of the CPSS-R direct-ionization theory with the present data apparently suggests that this theory is valid for L -shell ionization when $Z_1/Z_2 < 0.1$, and it should be applied with extreme caution for $Z_1/Z_2 > 0.1$.

IV. CONCLUSIONS

$L\alpha$ x-ray production cross sections have been determined for solid targets of ${}_{60}\text{Nd}$, ${}_{67}\text{Ho}$, and ${}_{79}\text{Au}$ that were thin enough that the target-thickness dependence of the x-ray yields was minimized. The x-ray production cross sections were found to be essentially independent of projectile charge state for ${}^{19}\text{F}$, ${}^{28}\text{Si}$, and ${}^{35}\text{Cl}$ projectiles without K -shell vacancies. For projectiles with K -shell vacancies, enhancements of the target $L\alpha$ x-ray cross sections were observed due to target L -shell vacancy production caused by electron capture to the K -shell of the projectile. From the projectile charge-state dependence of the $L\alpha$ x-ray cross sections, both DI and EC contributions have been extracted for comparison with Coulomb

ionization theories.

The EC contributions to the ionization cross sections were compared to the Nikolaev OBK approximation¹⁰ and the EC theory of Lapicki and Losonsky⁹ with the modification for a reduced binding effect by McDaniel *et al.*¹³ The Nikolaev OBK calculations overpredict the data by at least an order of magnitude in all cases, whereas the theory developed in Refs. 9 and 13 provides very good agreement with the EC data without the use of empirical scaling factors.

The DI cross sections were compared to the PWBA¹⁴ and the CPSS theory⁶ after the nonrelativistic predictions of both of these theories were multiplied by relativistic (R) correction factors.²² The PWBA-R reproduced the projectile Z_1 dependence of the data but overpredicted the data by increasing amounts with increasing Z_2 of the target. The PWBA-R theory gave the best agreement with the data for the largest ratios of Z_1/Z_2 , whereas the CPSS-R theory underpredicted the data with increasing Z_1/Z_2 . It appears that the CPSS theory for direct L -shell ionization is valid only when $Z_1/Z_2 < 0.1$ although the experimental x-ray data may not be simply related to the L -shell vacancy cross sections through the standard fluorescence and Coster-Kronig yields.²⁰ These yields would have to be increased when corrected for multiple ionization processes, which are of growing importance with increasing Z_1/Z_2 . The corrected yields might substantially reduce the differences in Fig. 6 between the present data and the CPSS-R predictions. They may also bring the electron capture

data even closer to the predictions of EC theory^{9, 13} (Figs. 2-4) at smaller v_1/v_{2L} where multiple ionization becomes increasingly important.

ACKNOWLEDGMENTS

We wish to acknowledge R. Mehta, A. Zander, T. Button, W. Holland, M. Andrews, K. Kuenhold, R. P. Chaturvedi, R. M. Wheeler, and L. A. Rayburn for their assistance with various phases of data acquisition. Special thanks go to W. T. Milner, E. Richardson, R. P. Cumby, F. Dicarolo, G. D. Alton, J. Johnson, and N. Ziegler for their assistance with the experimental facilities of the Tandem Accelerator Laboratory at ORNL. The authors would like to thank George Basbas for helpful discussions. One of us (S.R.W.) was supported by the Oak Ridge Associated Universities Graduate Fellowship from the Solid State Division, ORNL, Oak Ridge, Tenn. Work at North Texas State University (NTSU) was supported by the Research Corporation, the NTSU Organized Research Funds, and the Robert A. Welch Foundation. Acknowledgment is made to the Donors of the Petroleum Research Fund administered by the American Chemical Society for partial support of this research. Travel support to ORNL provided by Oak Ridge Associated Universities. Research by one of us (P.D.M.) was sponsored by Division of Physical Research, U.S. Department of Energy under contract W-7405-eng-26 with Union Carbide Corporation. Work by one of us (G.L.) supported by the U.S. Department of Energy.

¹See, J. D. Garcia, R. J. Fortner, and T. M. Kavanagh, *Rev. Mod. Phys.* **45**, 111 (1973); C. H. Rutledge and R. L. Watson, *At. Data* **12**, 195 (1973); G. Lapicki, Ph.D. thesis (New York University, 1975) (unpublished); T. L. Hardt and R. L. Watson, *At. Data* **17**, 107 (1976) for compilations of these data.

²C. G. Soares, R. D. Lear, J. T. Sanders, and H. A. Van Rinsvelt, *Phys. Rev. A* **13**, 953 (1976); J. R. Chen, *ibid.* **15**, 487 (1977); C. V. Barros Leite, N. V. de Castro Faria, and A. G. de Pinho, *ibid.* **15**, 943 (1977); S. R. Wilson, F. D. McDaniel, J. R. Rowe, and J. L. Duggan, *ibid.* **16**, 903 (1977).

³W. Brandt, R. Laubert, and I. Sellin, *Phys. Rev.* **151**, 56 (1966); G. Basbas, W. Brandt, and R. Laubert, *Phys. Rev. A* **7**, 983 (1973).

⁴G. Basbas, W. Brandt, and R. Laubert, *Phys. Rev. A* **17**, 1655 (1978).

⁵W. Brandt and G. Lapicki, *Phys. Rev. A* **10**, 474 (1974).

⁶W. Brandt and G. Lapicki (to be published).

⁷J. R. Macdonald, L. Winters, M. D. Brown, T. Chiao, and L. D. Ellsworth, *Phys. Rev. Lett.* **29**, 1291 (1972); J. R. Mowat, D. J. Pegg, R. S. Peterson, P. M. Griffin, and I. A. Sellin, *ibid.* **29**, 1577 (1972).

⁸J. R. Macdonald, L. M. Winters, M. D. Brown, L. D. Ellsworth, T. Chiao, and E. W. Pettus, *Phys. Rev. Lett.* **30**, 251 (1973); J. R. Macdonald, P. Richard, C. L. Cocke, M. Brown, and I. A. Sellin, *ibid.* **31**, 684 (1973); L. M. Winters, J. R. Macdonald, M. D. Brown, T. Chiao, L. D. Ellsworth, and E. W. Pettus, *Phys. Rev. A* **8**, 1835 (1973).

⁹G. Lapicki and W. Losonsky, *Phys. Rev. A* **15**, 896 (1977). These calculations, contrary to the claims made in the literature [see C. D. Lin, *J. Phys. B* **11**, L185 (1978); C. D. Lin, S. C. Soong, and L. N. Tunnell, *Phys. Rev. A* **17**, 1646 (1978)], were performed without any semiempirical corrections.

¹⁰V. S. Nikolaev, *Zh. Eksp. Teor. Fiz.* **51**, 1263 (1966) [*Sov. Phys.-JETP* **24**, 847 (1967)].

¹¹J. R. Oppenheimer, *Phys. Rev.* **31**, 349 (1928).

¹²H. C. Brinkman and H. A. Kramers, *Proc. Acad. Sci. (Amsterdam)* **33**, 973 (1930).

¹³F. D. McDaniel, J. L. Duggan, G. Basbas, P. D. Miller, and G. Lapicki, *Phys. Rev. A* **16**, 1375 (1977).

¹⁴B.-H. Choi, E. Merzbacher, and G. S. Khandelwal, *At. Data* **5**, 291 (1973).

¹⁵J. T. Routti and S. G. Prussin, *Nucl. Instrum. Methods*

- 72, 125 (1969).
- ¹⁶F. D. McDaniel, J. L. Duggan, P. D. Miller, and G. D. Alton, *Phys. Rev. A* 15, 846 (1977).
- ¹⁷T. J. Gray, P. Richard, K. A. Jamison, J. M. Hall, and R. K. Gardner, *Phys. Rev. A* 14, 1333 (1976).
- ¹⁸F. D. McDaniel, T. J. Gray, and R. K. Gardner, *Phys. Rev. A* 11, 1607 (1975); F. D. McDaniel, T. J. Gray, R. K. Gardner, G. M. Light, J. L. Duggan, H. A. Van Rinsvelt, R. D. Lear, G. H. Pepper, J. W. Nelson, and A. R. Zander, *ibid.* 12, 1272 (1975).
- ¹⁹B. L. Doyle, U. Schiebel, J. R. Macdonald, J. Trow, J. A. Guffey, and L. D. Ellsworth, *Bull. Am. Phys. Soc.* 21, 1248 (1976); I. A. Sellin, *Adv. At. Mod. Phys.* 12, 215 (1977).
- ²⁰M. O. Krause, *J. Phys. Chem. Ref. Data* 8, No. 2 (1979).
- ²¹J. H. Scofield, *Phys. Rev. A* 10, 1507 (1974).
- ²²J. S. Hansen, *Phys. Rev. A* 8, 822 (1973).